The Seoul Journal of Medicine
Vol. 27, No. 3:211-231, September 1986

Membrane Currents in the Atrioventricular Node of the Rabbit†

Won Kyung Ho, Woo Gyeum Kim and Yung E Earm

Department of Physiology, College of Medicine
Seoul National University, Seoul 110, Korea

=Abstract=The rabbit AV node was isolated and dissected into small strips of 0.3 mm width to apply two microelectrode voltage clamp technique. Then, slow inward current (i_{si}), hyperpolarization activated inward current (i_f) and pump current were recorded and their kinetic properties were analysed.

The results obtained were as follows:

1. The isolated AV node continued to beat, but the rate was slower than that in the SA node. The configuration of action potential showed regional difference. Small AV node preparations also showed spontaneous action potentials whose configurations were similar to those in the SA node. Resting membrane potential was about -40 mV.

2. On depolarization from the holding potential of -40 mV to various potential level, slow inward current (i_{si}) was recorded. It was disappeared by adding 2 mM Mn^{++} and increased remarkably by 10^{-6}M adrenaline. Current-voltage relationship, steady-state inactivation and recovery from inactivation were also studied and considered similar to those in other cardiac tissues.

3. In response to hyperpolarizing voltage clamp pulse, the current i_f was activated. The reversal potential was about -25 mV. 0.5 mM Cs^+ decreased i_f in a voltage-dependent manner. 10^{-6}M adrenaline showed little effect on i_f.

4. The activity of electrogenic Na^+ pump was demonstrated by K^+-induced transient outward current or transient hyperpolarization after pre-treatment with K^+-free Tyrode solution. The pump activity was affected by duration of pre-treatment, K^+ concentration in recovery solution and Ca^{++} concentration in K^+-free Tyrode solution.

Key words: *Two microelectrode voltage clamp technique, Slow inward current, Hyperpolarization activated inward current, Pump current, AV node*

INTRODUCTION

The atrioventricular node has been considered as the sole pathway of the impulse propagation from the atrium to the ventricle. Delayed conduction in the AV node makes the heart function as an efficient pump. Also it serves as a filter which prevents as excessive number of impulses from reaching the ventricle during supraventricular tachycardia (Leclercq and Coumel 1983). In addition, the AV node has the automaticity and acts as a subsidiary pacemaker of the heart when the SA node fails to control the cardiac rhythm (Watanabe and Dreifus 1968). In spite of these essential physiological functions of the AV node, the underlying ionic mechanism remains unclear and informations on the current system have been obtained mostly by analysis of the action potential.

The AV nodal cell was first impaled with mic-

†This study was supported by research grant from Korea Science and Engineering Foundation (1983) and grant for assistant from College of Medicine, Seoul National University.

roelectrode in 1957 (Hoffman *et al.* 1958) followed by the demonstration of the nodal delay associated with a slow waveform of the action potential (Hoffman *et al.* 1959). Using TTX and Mn^{++}, Zip and Mendez (1973) suggested that the slow inwa current was responsible for the slow action potei tial in N cells (Paes de Carvalho and Almeid 1960) of the AV node. It was also supported b experiments using acetylcholine (Ten-Eick *et a* 1976), catecholamine (Rougier *et al.* 1969) anc Ca^{++} channel blocker (Wit and Cranefield 1974) However, existence of TTX-sensitive upstroke component was also reported by Ruiz-Ceretti and Ponce Zumino (1971).

In 1980, Kokubun *et al.* suggested that spontaneously active small AV node specimen (0.5 × 0.5 mm) served as an unique material for the study on the underlying mechanism of the spontaneous activity of AV node. Thereafter, Noma *et al.* (1980) and Kokubun *et al.* (1982) found that the voltage clamp technique used in the SA node cell could be applied to the small AV node preparation. They discovered the presence of various ionic current systems which were similar to those in other cardiac tissues, especially in the SA node. But further studies about channel properties and kinetic analysis of individual channel system are still necessary.

On the other hand, there have been arguments about cell coupling in the AV node. Its existence was denied by Pollack (1976), and high coupling resistance enough to explain very slow conduction was proposed by Lieberman *et al.* (1973). DeMello (1977) and Kokubun (1982) suggested that electrical coupling was fairly reasonable and electrotonic interaction between cells could occur. However, it is difficult to evaluate the importance of the electrotonic interaction as a factor involved in the function of the AV node. Furthermore, inhomogeneity of the AV node structure (Paes de Carvalho and Almeida 1960; Mendez and Moe 1966) seems to make the problem more complicated.

In the present study, the slow inward current (i_{si}), the hyperpolarization activated inward current (i_f) and the pump current in the AV node were demonstrated using two microelectrode voltage clamp technique and the kinetic analyses were performed.

MATERIALS AND METHODS

Preparation of AV node

Rabbits of either sex weighing about 1 Kg were used in the present experiment. Animals were killed by a blow on the hind neck and exsanguinated. Chest was opened, and heart was extracted quickly and transferred into a dissection chamber containing oxygenated Tyrode soluton.

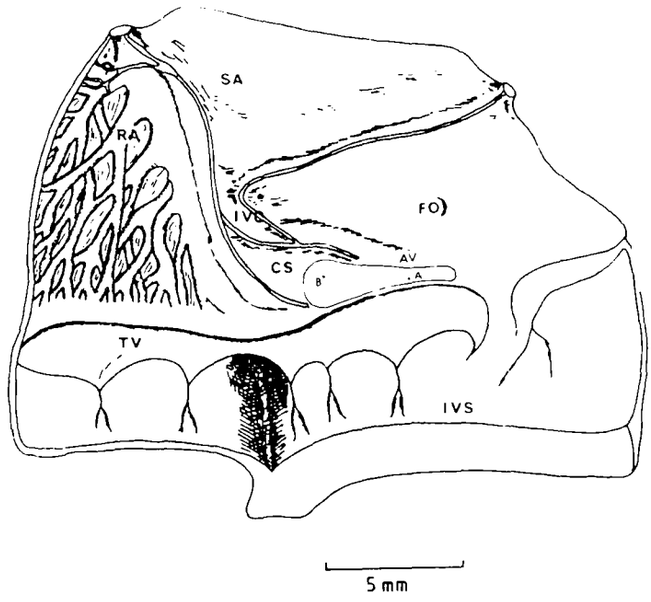

Fig. 1. AV node and surrounding structure. AV node is located between the ostium of the coronary sinus and the leaflet of the tricuspid valve. SA: sinoatrial node. IVC: inferior vena cava. FO: fossa ovalis. CS: opening of coronary sinus. AV: atrioventricular node. TV: tricuspid valve. IVS: interventricular septum (A: See Results Section 1).

Right atrium and part of right ventricle were separated from the rest of the heart and cut open through the atrioventricular orifice followed by the exposure of the AV node. The region between the ostium of the coronary sinus and the leaflet of the tricuspid valve was regarded as the AV node and its size was approximately 5 mm × 3 mm. It was dissected along the dashed line shown in Fig. 1 with fine scissors. The isolated AV node usually continued to beat spontaneously. After the recovery for one hour, the specimen was used either for observation of action potential and its conduction or for the following procedure to make small strips for the voltage clamp study.

With a fine razor blade, the isolated AV node was cut parallel to the tricuspid valve into 2 or 3 strips of 0.5 mm width. These strips were further dissected to the reduced width of about 0.3 mm. These small strips did not show spontaneous activity for a while but followed this with resumption of beating.

In one hour, two ligatures were tied around a beating portion using unravelled fine cotton thread to produce a preparation with a tiny node of approximately 0.3 mm in length and 0.3 mm in width. This small preparation was placed in experimental chamber which was being perfused with oxygenated Tyrode solution, and was held by fine entomological pins and a tungsten wire loop.

Experimental chamber and temperature control

Experimental chamber, internal dimesions of which were 22mm× 9mm×3mm, was made of Perspex. Through drippers, its inlet was connected with the solution bottle and the outlet with the suction apparatus. The chamber was electrically isolated from solution bottle and outflow stream by using drippers.

The solution bottle had a water jacket which was connected with constant temperature circulator bath (Haake FE). The flow rate was set to about 1 ml per minute by the height of solution bottle.

Experimental temperature was maintained at about 35°C and monitored with thermistor before every experiment.

Voltage clamp technique

A two microelectrode voltage clamp method was used. The current was measured with Ag/AgCl electrode in the bath connected to virtual ground amplifier. The voltage was measured with a 3M-KCl filled glass microelectrode. As an indifferent electrode, Ag/AgCl electode was used. The voltage clamp apparatus had two voltage outputs. This made it possible either to record voltages from two microelectrodes, or to use one microelectrode as a current injector and another as a voltage recorder. Results were recorded on a pen-recorder (Devices). An oscilloscope (Advance) was used to display the results during the experiment. For recording voltage and passing currents, glass microelectrodes were made by pulling fibre-filled borosilicate capillary tubes with external diameter of 1.5 mm with a vertical type electromagnetic puller (Narishige). The current passing electode was bevelled from an initial resistance of 45 MΩ to 15 MΩ in a thick slurry beveller containing 20% alumina in 3 M KCl.

A current injecting electrode was inserted as centrally as possible in the preparation so that the voltage drops in the periphery would be minimal. Another microelectrode for voltage recording was inserted as near the first electrode as possible. When the preparation was spontaneously active, the two microelectrodes showed completely superimposable voltage recordings.

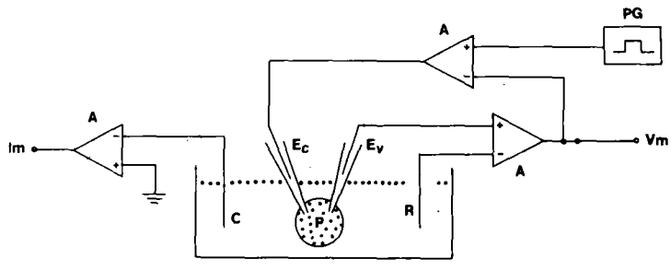

Fig. 2. Simplified scheme of the electrical circuit for voltage clamp. A: amplifiers. R: Ag/AgCl reference electrode. C: Ag/AgCl current recording electrode. Ec: glass-microelectrode for current injecion. Ev: glass-microelectrode for voltage recording. P: preparation, PG: pulse generator. Vm: membrane voltage. I_m: membrane current.

When the preparation was clamped, the squareness of membrane potential in response to commanding pulses was considered as success of the experiment. The voltage was held at zero-current level which was mostly around -40 mV.

The electrical circuit for voltage clamp was shown schematically in Fig. 2.

Solutions

Normal Tyrode solution contains NaCl 140 mM, KCl 3 mM, $CaCl_2$ 2 mM, $MgCl_2$ 1 mM, Dextrose 5 mM. With 5 mM Tris-HCl, pH was adjusted to 7.4 at 35°C.

In order to control K^+ concentration in the range of 0-13 mM, K^+ was simply removed from or added to normal Tyrode solution.

Drugs or chemicals used in this experiment were adrenaline, isoprenaline, diltiazem, ouabain, CsCl and $MnCl_2$.

RESULTS

1. Spontaneous action potentials

When the AV node was isolated, it usually continued to beat. The rate of spontaneous beat was in the range of 50-60 per minute, which was slower than that of SA node.

Action potentials were recorded from two points simultaneously, and their conduction pattern in the isolated AV node was able to be estimated by using one point as reference. Action potential was initiated in region A (Fig. 1) which seemed to be NH region. Then, it spreaded through the node in retrograde direction with the conduction velocity of about 0.05m/second.

The action potentials in various regions showed

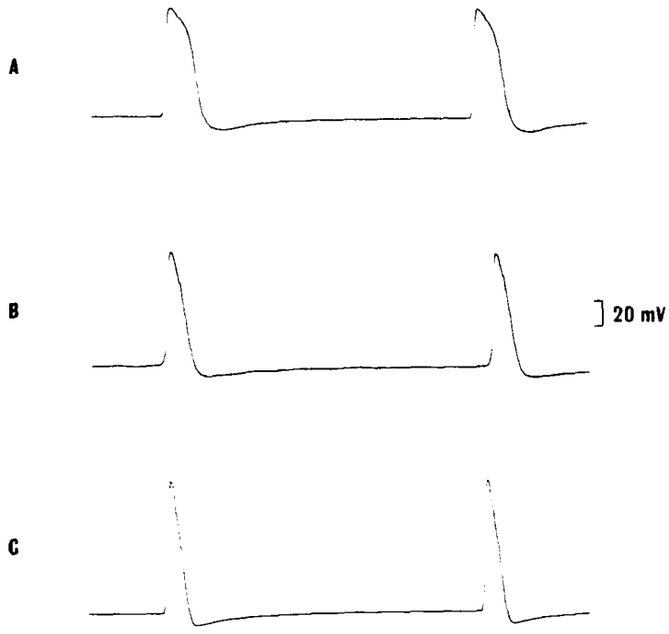

Fig. 3. Action potenitials recorded in various areas of the isolated AV node. A, B and C seem to correspond to NH, N and AN region, respectively.

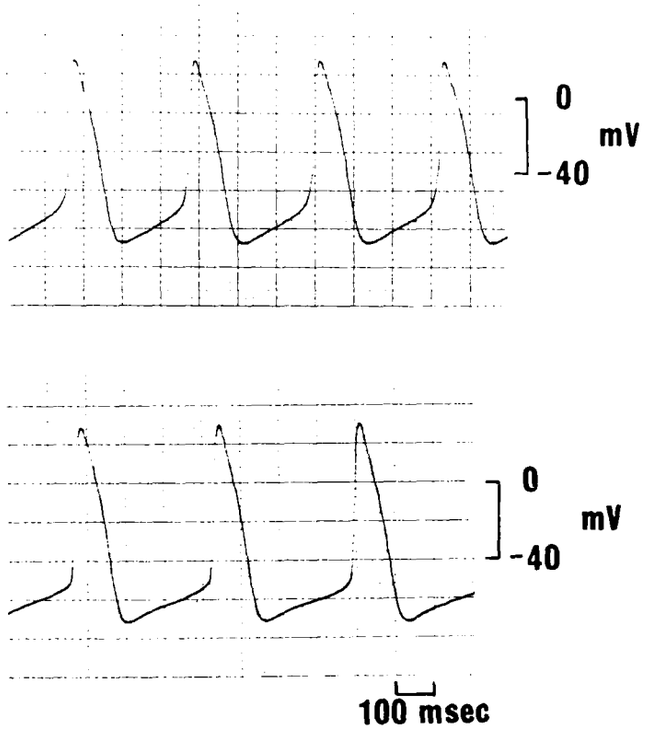

Fig. 4. Action potentials in small AV node preparation. It appears similar to the action potential of the SA node.

different configurations. The action potentials shown in Figs. 3A, 3B and 3C were regarded as those of the node-His (NH), nodal (N) and atrionodal (AN) region, respectively.

When the AV node was dissected into small strips, each part resumed beating in a few minutes. A few examples of the action potentials in small AV node strips were shown in Fig. 4. The average rate was 150/min and it was faster than 50/min in the isolated whole AV node. The configuration of action potential was different from that in Fig. 3. They showed larger pacemaker potential, and the overall configuration was similar to that of action potential in the SA node. The average values were as follows: amplitude 96 mV, maximum diastolic potential -70 mV, overshoot +26 mV. It seemed that regional difference found in isolated AV node was abolished after dissection.

2. Resting membrane potential

Resting membrane potential in spontaneously active cell was estimated in two ways. Firstly, the potential of zero-current level at which the clamp was performed was measured. Secondly, spontaneous activity was ceased by Ca^{++} channel blocker, 5×10^{-6}M diltiazem. Resting membrane potentials measured by two methods appeared to be similar and around -40 mV.

Sometimes, spontaneous beating was not found. In the quiescent preparation, resting membrane potential (RMP) seemed to be more negative and around -50 mV.

The effect of K^+ concentration on RMP was studied using the quiescent preparation. Change of the perfusate from normal Tyrode to 1 mM K^+-Tyrode solution made RMP hyperpolarized by 9 mV. By increasing K^+ concentration from 1 mM to 43 mM step by step, RMP became depolarized by 36 mV.

The relationship of the outside concentration of K^+ and RMP was plotted in semilog paper and shown in Fig. 5. RMP was little changed in response to change of K^+ concentration in the range of 1-23 mM. Then, the curve was far deviated in the direction of the depolarization from the line predicted by Nernst equation.

3. Slow inward current (i_{si})

The slow inward current was investigated by the application of step depolarization from holding potential of -40 mV in small AV node specimen (Fig. 6).

This holding potential was chosen for the pur-

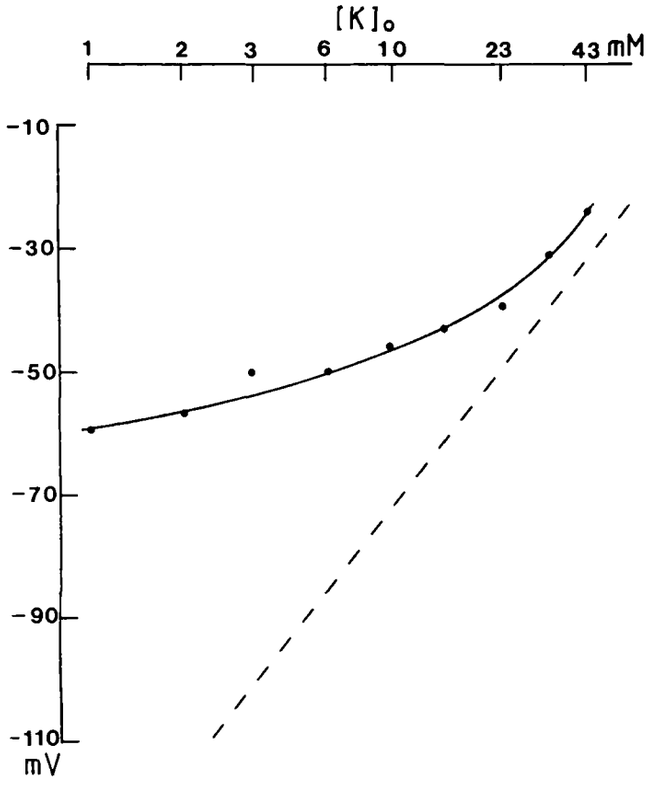

Fig. 5. Relationship between resting membrane potential (RMP) and K^+ concentration. Dotted line represents the theoretical one predicted by Nernst equation. Abscissa: K^+ concentration (mM) in semilog scale. Ordinate: resting membrane potential (mV).

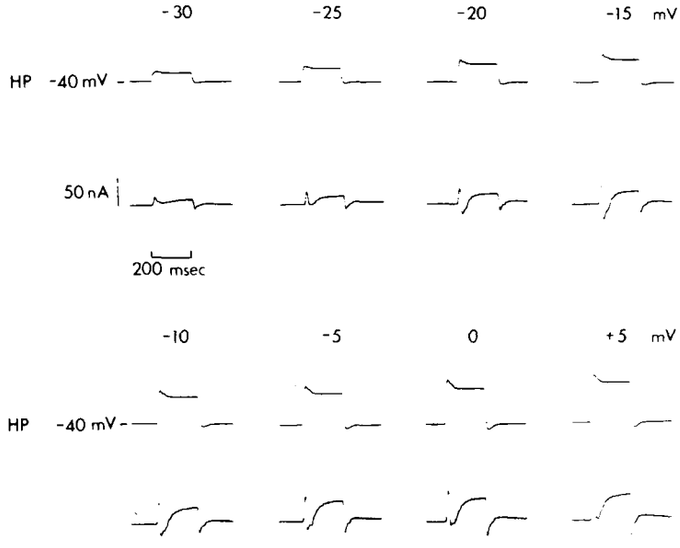

Fig. 6. Membrane currents in AV node in response to depolarizing voltage clamp pulses in normal Tyrode solution (Upper trace: voltage recording, Lower trace: current recording). Pulse duration is 200 msec. The numbers above the figure represent voltage level of the test pulse.

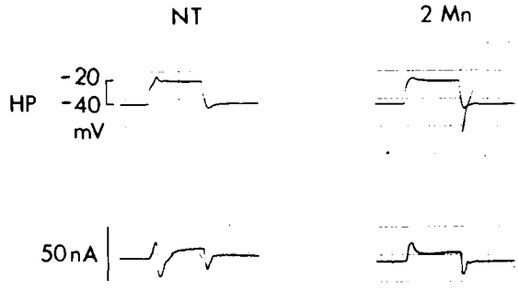

Fig. 7. Mn^{++} effect on i_{si} in AV node. Slow inward current in normal Tyrode solution (NT) is abolished by addition of 2 mM Mn^{++}.

pose of inactivating the fast inward Na current (Noma *et al.* 1977; Colatsky 1980; Brown *et al.* 1981).

On depolarization to -25 mV, outward capacitive current was followed by activation of inward going current which became inactivated soon. In succession, outward current was activated and reached steady level. The magnitude of inward current increased when test pulse was increased to -15 mV, and then decreased on further depolarization. This inward going current change was abolished by 2 mM Mn^{++} (Fig. 7). Therefore, it could be regarded that this current system in the AV node was same as the slow inward current (i_{si}) recorded in other tissues (Beeler and Reuter 1970; Noma *et al.* 1977).

Current-voltage relationship

From the results of Fig. 6, current-voltage relationship of i_{si} was plotted in Fig. 8. Open circles indicated the maximum inward current or minimum outward current during the various depolarizing test pulse. General contour showed typical bell shaped relation. Closed circles indicated the current amplitude at the end of the test pulse. These represented activation of outward potassium current, which increased as the test pulse became more positive.

Since the current change of i_{si} overlapped the outward current activation, it was difficult to determine the current magnitude of pure i_{si}. In this study, it was regarded that outward current was little activated at 100 msec after application of depolarization step. Then, the difference from the value at that time was considered as pure i_{si} (Isen-

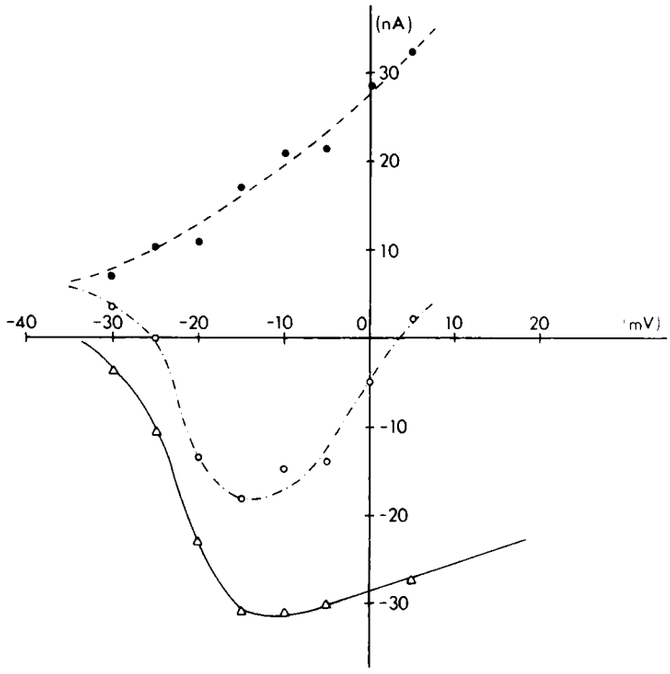

Fig. 8. Current voltage relationship of i_{si}. Open circle: Maximum inward current or minimum outward current in response to the various depolarizing pulse. Closed circle: current amplitude at the end of the test pulse. Triangle: pure inward current.

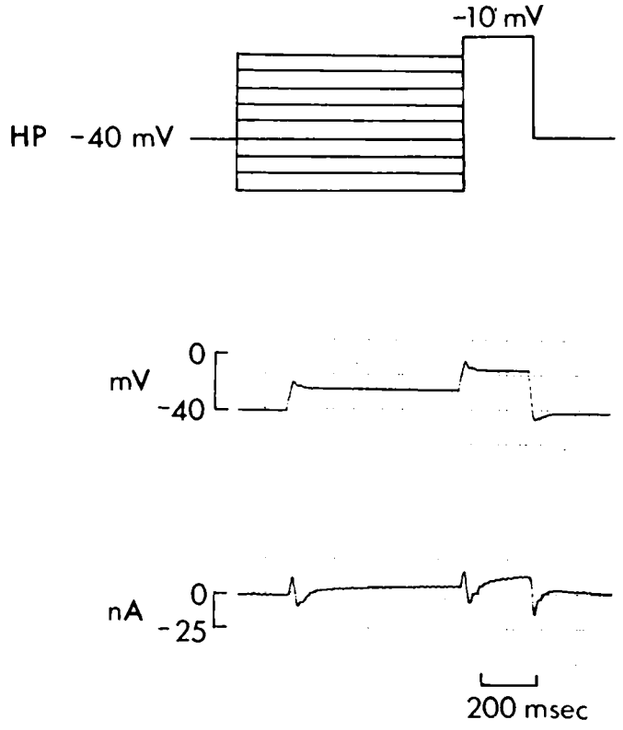

Fig. 9. The pulse protocol (top) to obtain the steady state inactivations of i_{si}. Conditioning prepulse for inactivating i_{si} is given from -55 mV to -15 mV by 5 mV step and 500 msec duration. One example of voltage clamp recording is shown in the bottom figure.

berg and Klöckner 1982; Coraboeuf 1980).

With this method, peak amplitudes of i_{si} at various test potential were measured and plotted in triangles. It was regarded as a true current-voltage relationship of i_{si} and appeared to cross abscissa at far positive potential.

Steady-state inactivation

In Fig. 9, the way to determine the steady-state value of inactivation parameter ($\bar{f}$) as the function of membrane potential was shown. The membrane was depolarized at different levels by conditioning prepulses long enough for the inactivation gate to reach its new steady-state of opening. Then, the second depolarizing pulse, which was sufficient to open the activation gate completely and allowed an inward current to cross membrane, was applied in succession. The amplitude of the inward current in response to the second pulse was considered to be proportional to the degree of opening of the inactivation gate at the end of the prepulse.

The ratio of the amplitudes of these currents to those without prepulses were regarded as $\bar{f}$ and plotted against the prepulse potential in Fig. 10.

The curve showed steep voltage dependency and reached 50% inactivation at -26 mV. The top

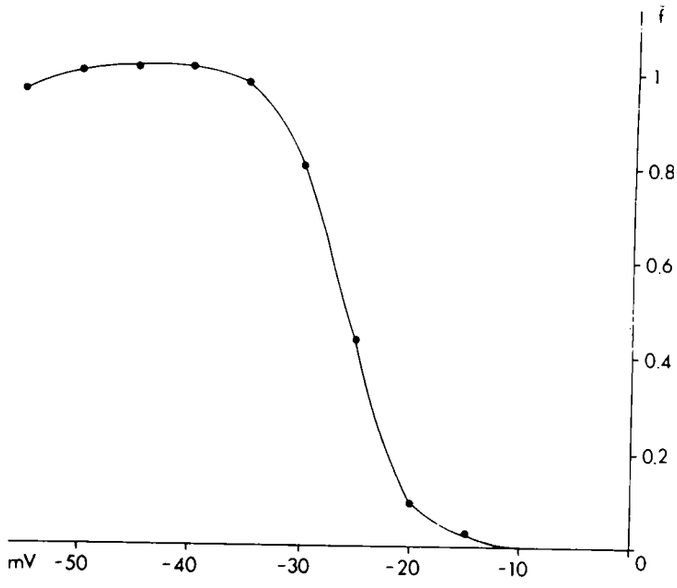

Fig. 10. Steady state inactivation ($\bar{f}$). Abscissa: membrane potential. Ordinate: fraction of the gate ($\bar{f}$) which remains open after inactivation reaches steady state by 500 msec prepulse.

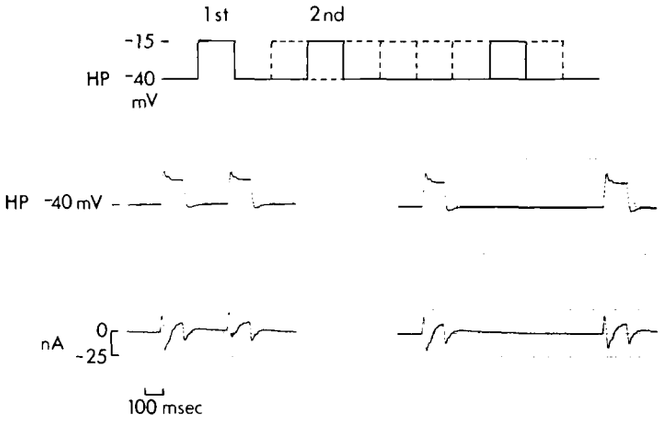

Fig. 11. Pulse protocol and two examples of current recording to observe the recovery process from inactivation.

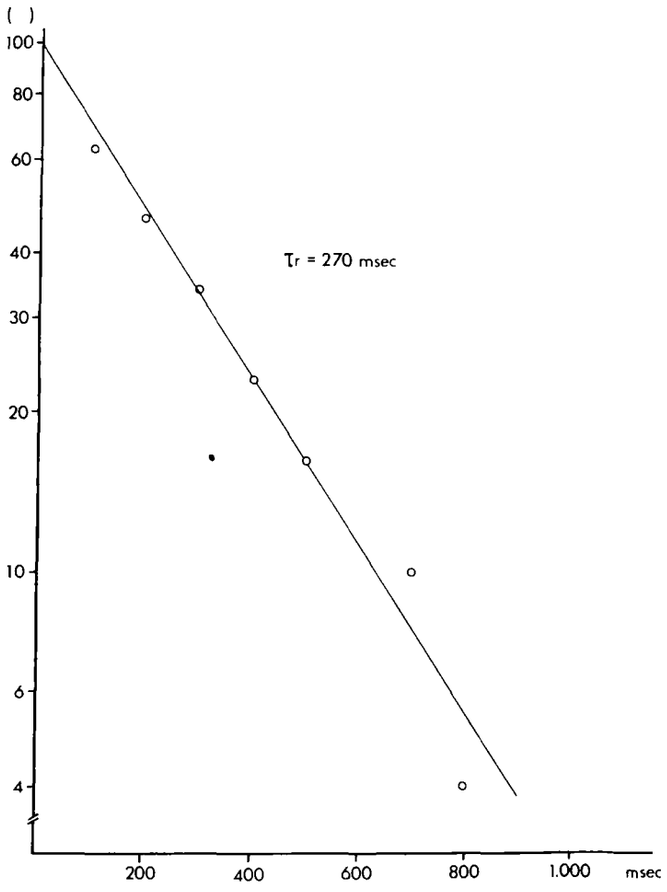

Fig. 12. Time course of removal of inactivation. It clearly showed that recovery from inactivation was also time-dependent and might obey first order kinetics.

of the curve bent slightly downward because the amplitudes of i_{si} decreased after the hyperpolarizing prepulses.

Removal of inactivation

In order that inactivated channel is used again, removal of inactivation process must be occurred. Considering the fact that the upstroke and the conduction of action potential in the AV node are contributed by i_{si}, the kinetics of recovery process might be important.

To find its time course, two identical depolarizing pulses separated by periods of repolarization of varying durations(d_r) were applied (Fig. 11). Then, the differences in amplitudes of i_{si} triggered by two pulses were measured and considered to indicate the degree of inactivation remained. In Fig. 12, these differences were plotted as a function of d_r on a semilogarithmic scale, and the time constant of the removal of inactivation (τ_r) could be determined at the given membrane potential between two pulses. It was 270 msec at -40 mV, which was close to the result of Kohlhardt *et al.* (1975) in the cat papillary muscle (τ_r was 300 msec at -10 mV).

Effect of adrenaline

In the small AV node preparation, adrenaline effect was manifested by the increase of the spontaneous discharge rate and the amplitude of action potential (Son 1985). To discover whether slow inward current was responsible for adrenaline action, the adrenalin effect on i_{si} in AV node was studied.

The results were shown in Fig. 13. The amplitude of i_{si} increased greatly, and the potential at which the amplitude of i_{si} reached a peak value became more negative (-25 mV) with 10^{-6}M adrenaline. The magnitude of current was so large in 10^{-6}M adrenaline solution that membrane potential was not well controlled. Therefore, quantitative comparison was impossible.

Outward shift of current at holding potential was also observed, which might contribute to the increase of maximum diastolic potential. Above changes were completely reversible (Fig. 13B).

Effect of Ca^{++}

Increase in i_{si} has been known to contribute to positive chronotropic effect. On the other hand, it has been reported that increase in Ca^{++} concentration made the spontaneous dischange rate slow in small preparations of SA node and AV node (Son 1985).

Current recordings at various depolarizing pulses in normal Tyrode solution and 6 mM Ca^{++}-Tyrode solution were shown in Fig. 14. In 6 mM Ca^{++}-Tyrode solution, i_{si} reached maximum value at -25 mV as in control, but decreased more rapidly than control. The maximum amplitude in 6 mM

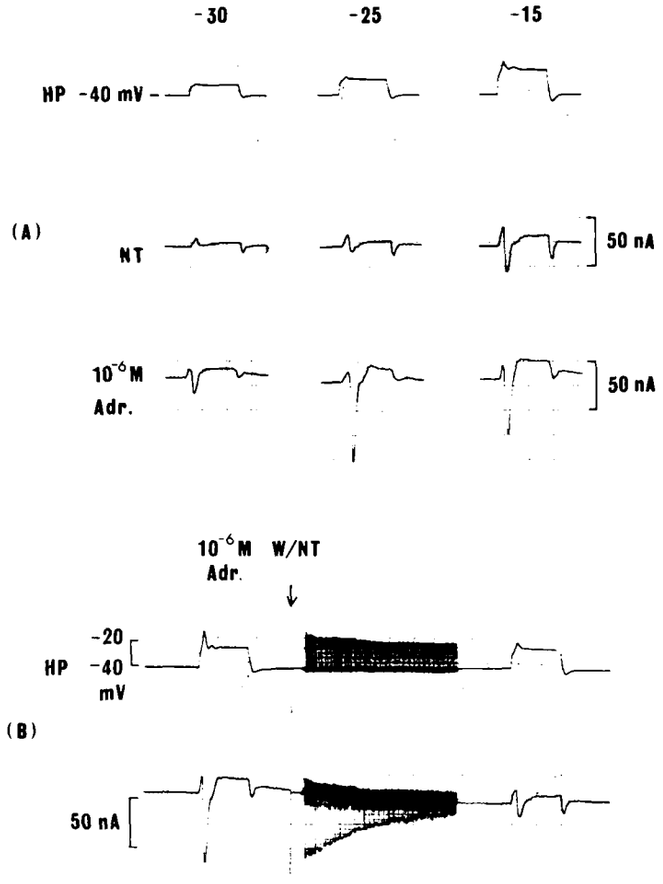

Fig. 13. Effect of adrenaline on i_{si}. A: Remarkable increase of i_{si} is seen by adding 10^{-6}M adrenaline. The numbers (-30, -25, -15) represent the potential of test pulse. Pulse duration: 200 msec. NT: normal Tyrode solution. B: The change is completely reversible by washing with normal Tyrode solution. Outward shift of holding current also returns to the control level.

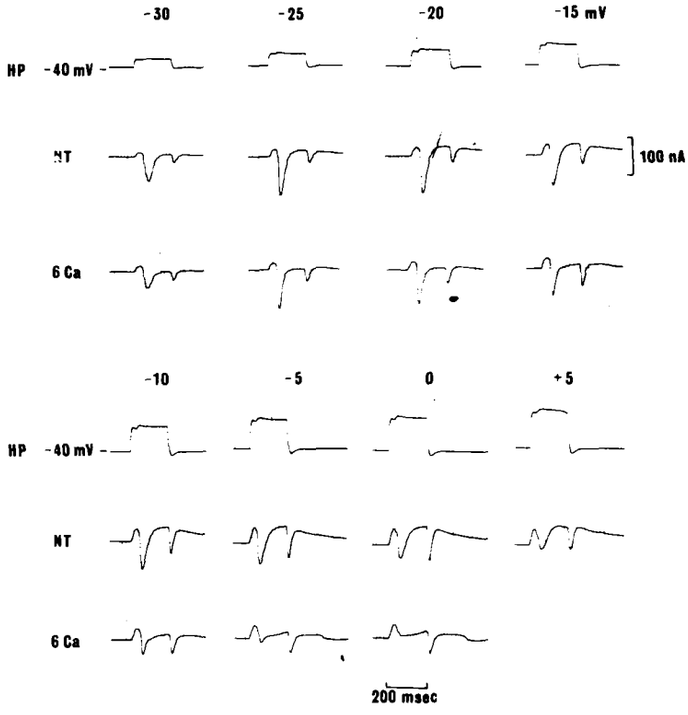

Fig. 14. Effect of Ca^{++} on i_{si}. The amplitude of i_{si} is decreased by 6 mM Ca^{++} when depolarization is over -10 mV.

Ca^{++} was almost same as that in control, and amplitude of current at further depolarization was much smaller in 6 mM Ca^{++}.

A curious response

During the voltage clamp study about i_{si}, some preparation showed different findings from the others. One of the cases was presented in Fig. 15, in which inward current was activated very slowly by step depolarization to -32 mV in the presence of 2 mM Mn^{++}. With the increase of the test pulse, the inward current appeared sooner. Whether this is a slow Mn^{++} curent or slow component of i_{si} (Noble 1984) is uncertain.

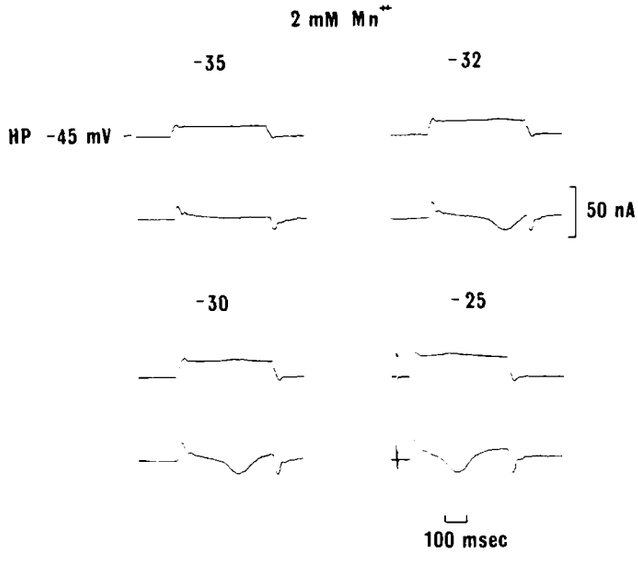

Fig. 15. One example of different response to depolarizing test pulse in the presence of 2 mM Mn^{++}.

4. Hyperpolarization activated current (i_f)

Kinetics of i_f

Currents in responses to hyperpolarizing voltage clamp pulses were shown in Fig. 16. From the holding potential of -40 mV, hyperpolarizing test pulses of 3 sec duration were applied in 10 mV step. A

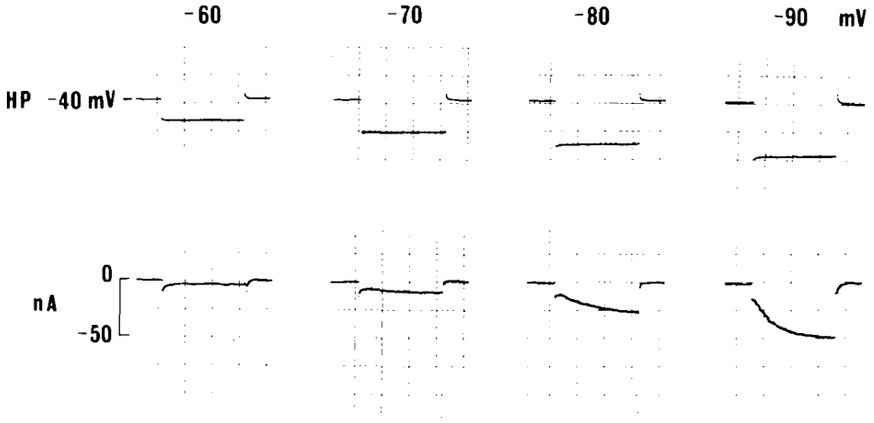

Fig. 16. Currents (lower trace) in response to hyperpolarizing voltage clamp pulses in normal Tyrode solution.

surge of inward capacitive current was seen at the beginning of each hyperpolarizing pulse followed by development of inward current in the voltage range negative to -70 mV. As the magnitude of the hyperpolarizing pulse was increased, the magnitude of current activation became larger in the inward direction and the time to reach the steady state was faster. The current did not show any tendency to reach a reversal potential at the maximum hyperpolarizing pulse which was near to K^+ equilibrium potential. At the end of each pulse, a surge of outward capacitive current was followed by the fast inward change which seemed to show the activation of i_{Na} and i_{si} and by slow deactivation tail current.

Above inward current activated by hyperpolarization was regarded as the same current system as i_f (Brown *et al.* 1980) or i_h (Yanagihara and Irisawa 1980) in SA node and designated as i_f in this study.

In most of the experiments, the amplitude of i_f in normal Tyrode was small and current tail was mixed with i_{Na} and i_{si} activation, which made the analysis of channel kinetics difficult. To circumvent the above problem, 2 mM Mn^{++}, 13 mM K^+-Tyrode solution was used. Fig. 17. showed i_f in 2 mM Mn^{++}, 13 mM K^+-Tyrode solution at various hyperpolarizing pulses. The result of this experiment was used for measurements of the time constant and steady state activation.

The magnitude of current due to i_f activation was attributed to total current change minus initial time independent step change. Steady state value was designated by i_{max}. The semilogarithmic plots of i_f activation during various hyperpolarization were shown in Fig. 18. The curves fitted single exponential well. The activation time constant was determined by the time during which the current change reached 63% of i_{max}. The time constant became shorter as the test pulse became more negative. It was 1,020 msec at -70 mV, 660 msec at -80 mV, and 370 msec at -90 mV. The time

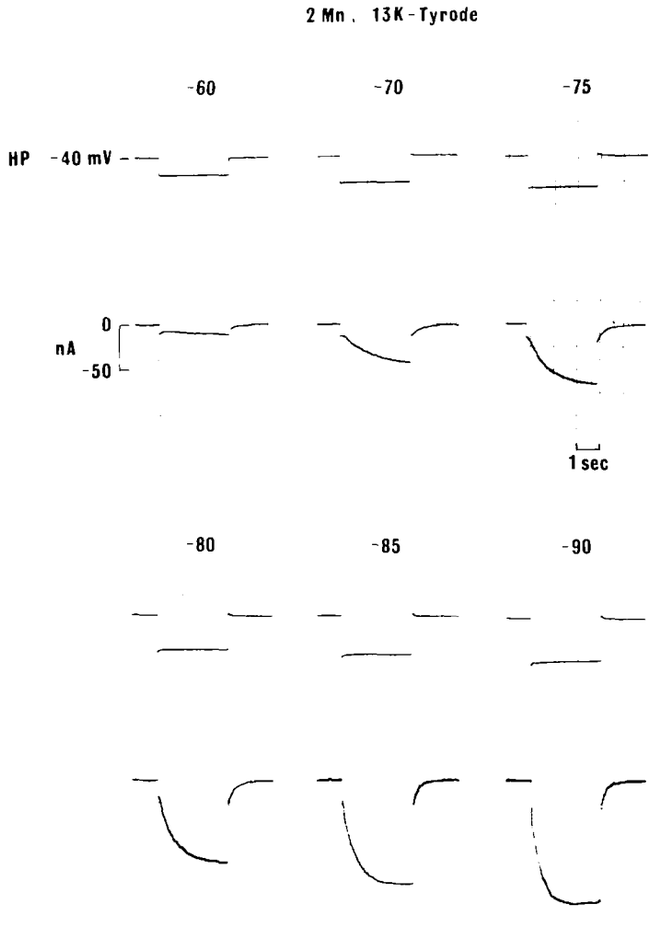

Fig. 17. Currents in response to hyperpolarizing voltage clamp pulses in 2 mM Mn^{++}, 13 mM K^+-Tyrode solution.

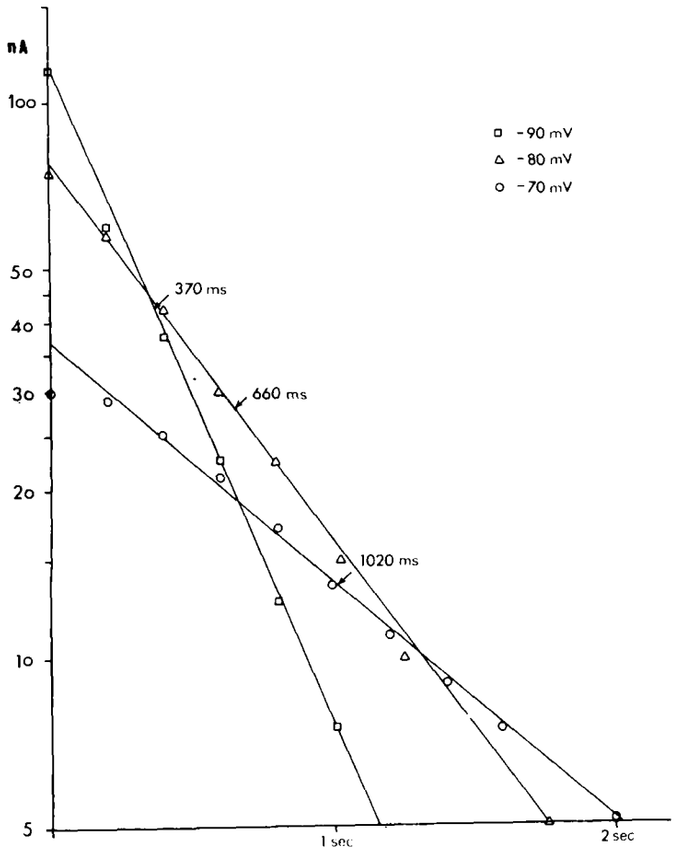

Fig. 18. Semilogarithmic plot of i_f current activation at different test pulse potentials. The curves fit single exponential well. Abscissa: duration of clamp pulse. Ordinate: membrane current.

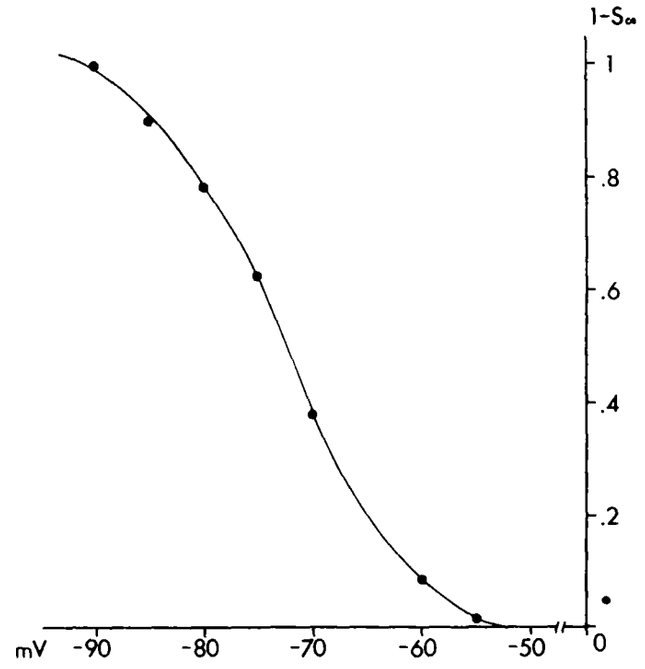

Fig. 19. Activation curve of i_f. Abscissa: test pulse potential. Ordinate: fraction of open gate at steady state ($1-s_{\infty}$).

constant of i_f in normal Tyrode solution, which was determined in only one case at -90 mV, was 800 msec. It was much longer than that in 2 mM Mn^{++}, 13 mM K^+-Tyrode solution.

To obtain steady state activation of i_f, which was designated as $1-s_{\infty}$, the amplitude of inward current tail was measured and its relative value to that at -90 mV was plotted against test pulse potential in Fig. 19. The result showed that the activation threshold was about -60 mV and 50% activation was obtained at about -74 mV.

Fully activated I-V relationship

The fully activated current-voltage realtionship for i_f was measured from the value of i_{max} and $1-s_{\infty}$. The amplitude of i_f at steady state was determined by the product of the fully activated current ($\bar{i}_f$) and $1-s_{\infty}$ at a given test pulse. Then,

$$i_{max}=\bar{i}_f\times(1-s_{\infty})$$

$$\bar{i}_f=i_{max}/(1-s_{\infty})$$

The values of i_{max} and $1-s_{\infty}$ were available from Fig. 17 and Fig. 19, respectively. The calculated value of $\bar{i}_f$ was plotted in Fig. 20. In this case, the points could fit a straight line, and the line crossed abscissa at -28 mV.

Reversal potential

The reversal potential is one of the important indicators of the ionic nature of a current system.

To observe the potential at which the direction of current tail was reversed, the membrane potential was returned to various potential after the test hyperpolarizing pulse (Fig. 21). At -30 mV, inward current tail was observed, and at -20 mV, current tail became outward decaying. At -25 mV the current decay was not observed in either direction and regared as reversal potential of i_f in 2 mM Mn^{++}, 13 mM K^+ -Tyrode solution. This observed value was quite similar to the estimated value from the fully activated I-V relationship.

Effect of Cs^+ on i_f

In Fig. 22, the effect of 0.5 mM Cs^+ on the same preparation in Fig. 17 was shown.

Initial current jump on hyperpolarizing test pulse was not affected, but slowly activated inward current was greatly reduced to 47%, 38% and 35% of control value at -70 mV, -80 mV and -90 mV, respectively. Not only the magnitude of activation but also the speed of activation were greatly reduced. Time constant of i_f activation was prolonged from 660 ms to 920 ms at -80 mV, and from 370

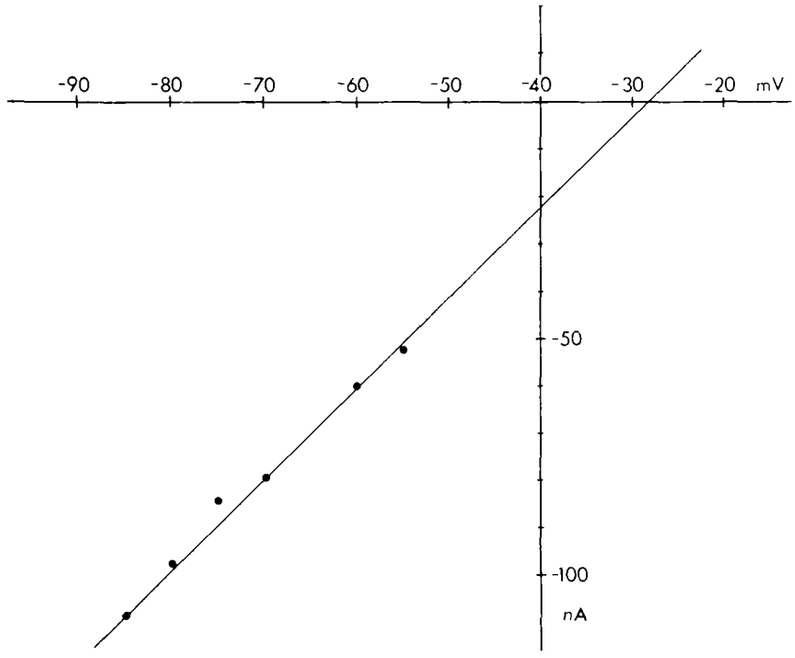

Fig. 20. Fully activated current-voltage relationship for i_f in 2 mM Mn^{++}, 13 mM K^+-Tyrode solution. The values were calculated by $i_{max}/(1-s)$, and fitted a straight line.

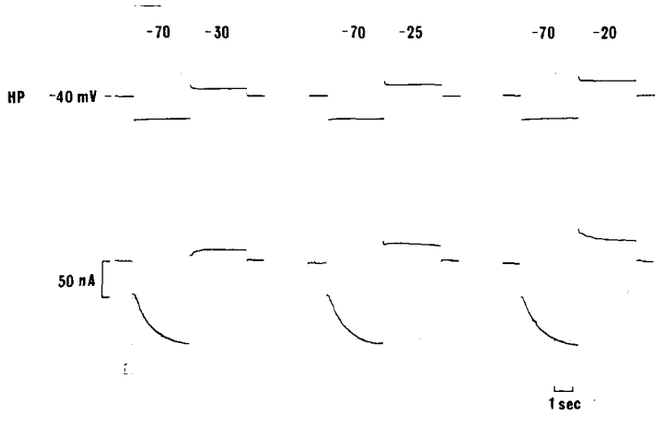

Fig. 21. Voltage clamp study to observe reversal potential of i_f. Returning to -25 mV, the current does not change in either direction. Upper trace: pulse protocol. Lower trace: current in response to each pulse.

msec to 750 msec at -90 mV.

Compared with the decrease of i_f activation, change in amplitude of tail was somewhat different. At -70 mV, the amplitude of tail in 0.5 mM Cs^+ was only 43% of that in control. At -80 mV and -90 mV, it was 66% and 85% of the control, respectively.

Effect of isoprenaline

The current, i_f, has been known as a pacemaker current, but its small size and slow time course of development in the pacemaker range have cast doubt on the extent to which i_f contributed to pacemaker activity.

On the other hand, adrenaline has a potent positive chronotropic effect on the AV node. Knowing whether the adrenaline effect is attributed to increased i_f or not, may give a suggestion about the contribution of i_f to pacemaker activity.

In this experiment shown in Fig. 23, 10^{-6}M isoprenaline increased slightly the amplitude of i_f during hyperpolarizing test pulse to -60 mV and -70 mV. But at more negative pulse the current did not increase with isoprenaline. The time course of activation did not change significantly.

5. Pump current

The presence of electrogenic Na^+ pump in the AV node was observed and its general properties were investigated.

To stimulate Na pump, 13 mM K^+-Tyrode solution was reperfused after having treated with K^+-free Tyrode solution of 10 minutes.

In Fig. 24A, membrane current was recorded under the voltage clamp condition. Change of perfusate from K^+ -free to 13 mM K^+ -Tyrode solution resulted in transient increase of outward current followed by inward shift. It seemed that this current transient directly reflected the activity of an electrogenic Na^+ pump. Therefore it might be called as pump current.

Electrogenicity of Na^+ pump could be detected

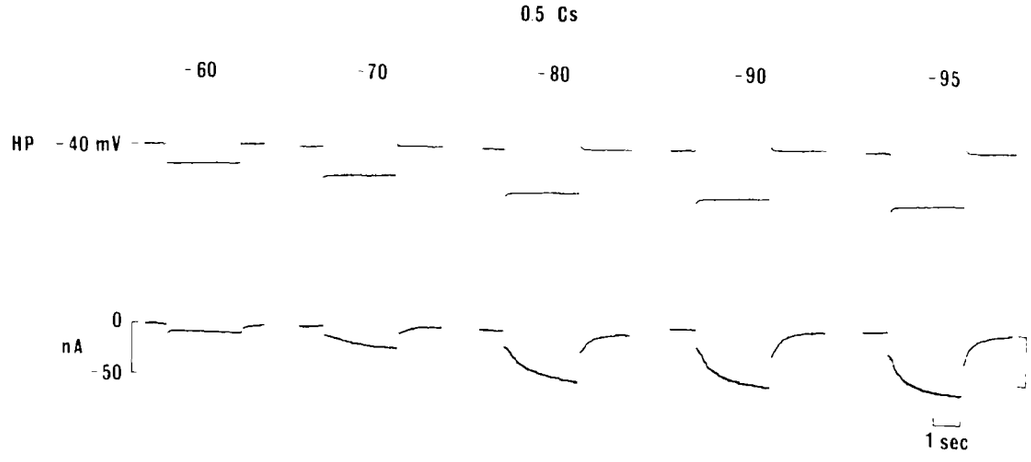

Fig. 22. Effect of 0.5 mM Cs^+ on hyperpolarization activated current.

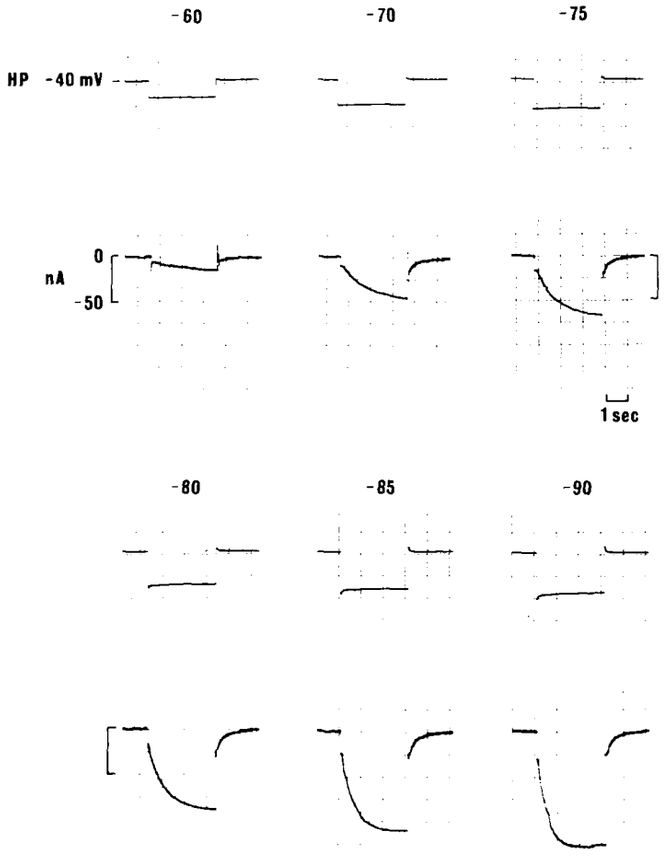

Fig. 23. Effect of 10^{-6}M isoprenaline on hyperpolarization activated current.

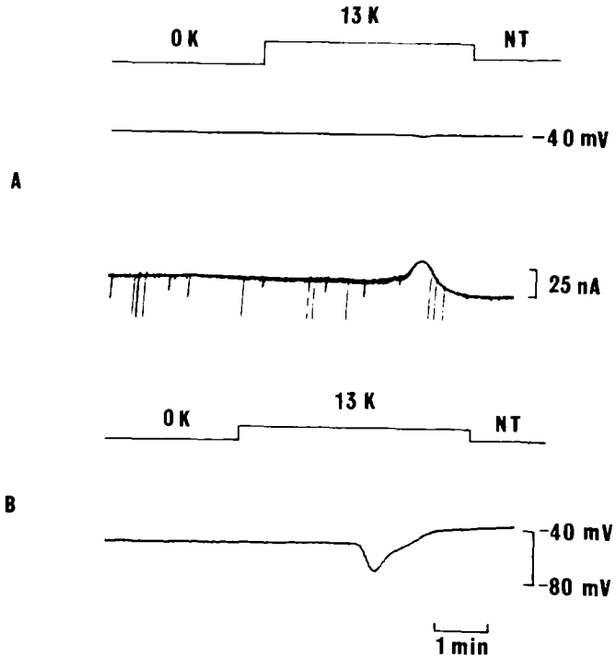

Fig. 24. Electrogenic Na^+ pump activity is revealed by pretreatment of K^+-free solution (OK) for 10 min. A: Under the voltage clamp condition, outward current transient resulted from 13 mM K^+-Tyrode solution (13K). B: In quiescent preparation made by adding 5×10^{-6}M diltiazem, same procedure was repeated. Transient hyperpolarization with the time course similar to that of current transient was noticed.

by recording transmembrane potential change which reflected underlying current change well if the current-voltage relatonship was linear. After the perfusate was changed from K^+-free to 13 mM K^+-Tyrode solution, AV node cell hyperpolarized beyond the steady state value by 20 mV. This hyperpolarization was followed by depolarization to the control resting potential within a few minutes (Fig. 24B).

The time course of this transient hyperpolariza-

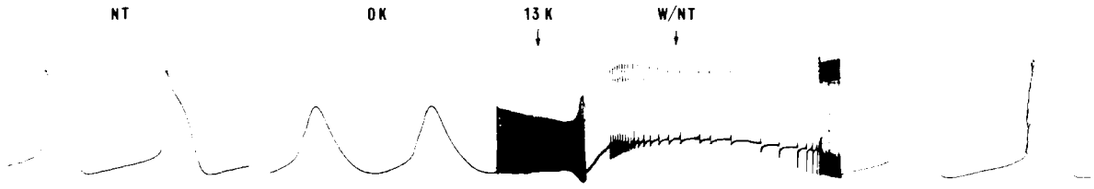

Fig. 25. K^+-induced hyperpolarization in spontaneously active AV nodal cell. Transient hyperpolarization followed by depolarization to new steady level in 13 mM K^+-Tyrode was seen.

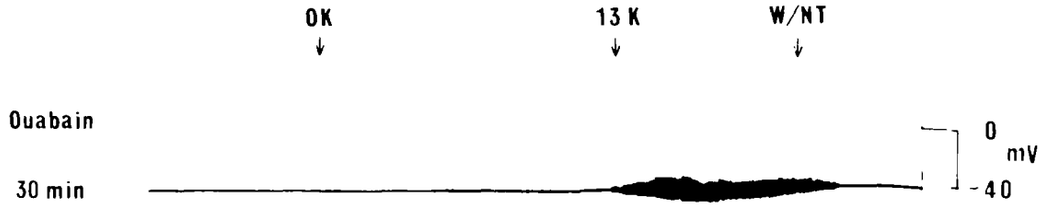

Fig. 26. Ouabain effect on K^+-induced hyperpolarization. Transient hyperpolarization as shown in Fig. 24B was not found.

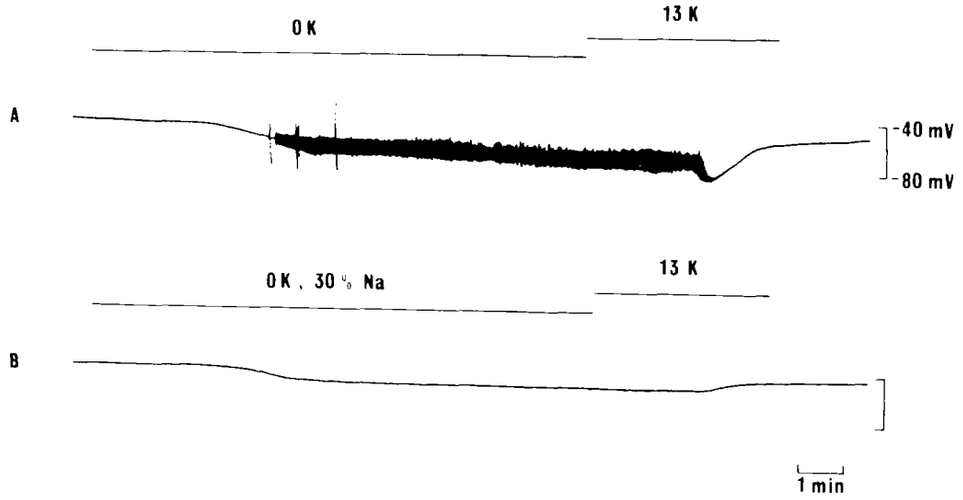

Fig. 27. Effect of decreasing Na^+ concentration. A: control recording showing K^+-induced transient hyperpolarization. B: Pre-treated with K^+-free, 30% Na (70% Na^+ was substituted by Tris) Tyrode solution, transient hyperpolarization was not found.

tion was very similar to that of current transient. It was observed in both the spontaneous active cells (Fig. 25) and the quiescent cells which were made by adding 5×10^{-6}M diltiazem.

To prove that electrogenic sodium pump was responsible for this transient hyperpolarization, the preparation was treated with 10^{-6}M ouabain for 30 minutes and above procedures were repeated. As shown in Fig. 26, transient hyperpolarization was not found. Therefore, two other procedures known to inhibit the Na pump were employed: decreasing Na concentration (substituted by Tris) and cooling the tissue (Keynes and Swan 1959; Thomas 1972).

After recording a control of K^+-induced hyperpolarization in a quiescent AV node cell (Fig. 27A), the same cell was pretreated with K^+-free, 30%

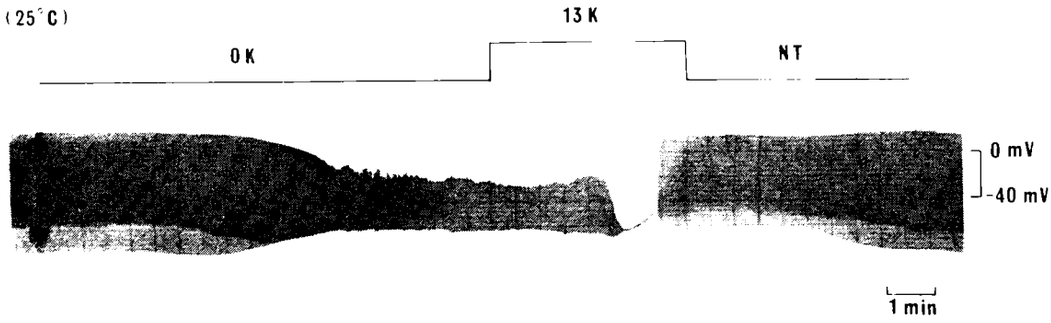

Fig. 28. Effect of low temperature. Lowering temperature from 35°C to 25°C, K^+-induced hyperpolarization is decreased remarkably.

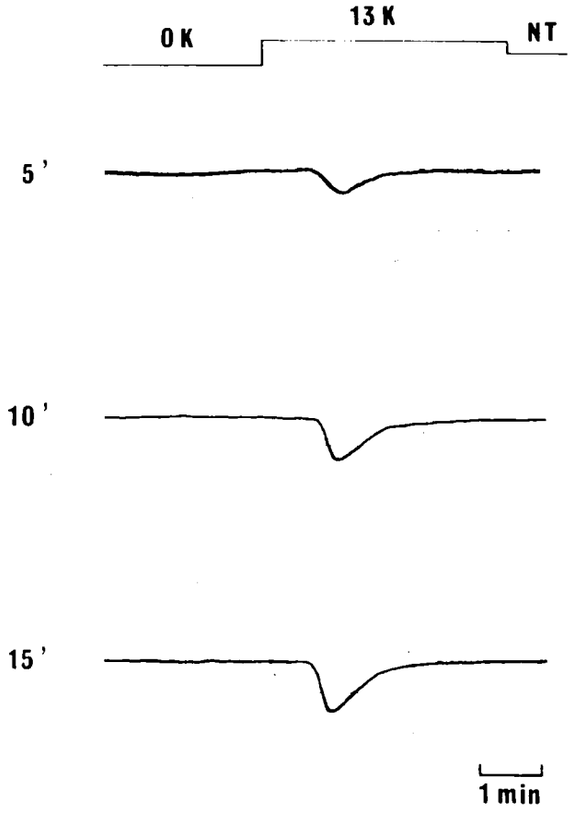

Fig. 29. Effect of the duration of pre-treatment with K^+-free Tyrode. The periods of pre-treatment were 5 min (upper), 10 min (middle) and 15 min (lower), respectively. The amplitude of transient hyperpolarization increased with prolonging the pre-treatment.

Na^+-Tyrode (Fig. 27B). Change of the perfusate to 13 mM K^+-Tyrode solution did not result any transient hyperpolarization. Fig. 28 showed effect of low temperature on the transient hyperpolarization in the spontaneously active cell. At 25°C transient hyperpolarization as shown in Fig. 25 was hardly seen.

Effect of the duration of pre-treatment

It has been well known that the rate of Na^+ extrusion by the Na^+ pump increased following the increase of internal Na^+ concentration and saturation occurred at high internal Na^+ concentration (Thomas 1972).

To find the effect of $[Na^+]_i$ on Na^+ pump activity, duration of pre-treatment by K^+-free Tyrode solution was varied. As shown in Fig. 29, the amplitude of hyperpolarization increased by 16, 28 and 32 mV when pre-treatment period was 5, 10 and 15 min, respectively. The rate of hyperpolarization also increased.

Effect of K^+ concentration in recovery solution

For the activation of Na^+ pump, certain kinds of external cation, so called activator cation, were required. There are K^+, Rb^+ and NH_4^+, for example. Increasing the concentration of activator cation was expected to cause promotion of Na^+ extrusion.

When K^+ concentration in recovery solution was increased from 1 mM to 3, 13, 23 mM after 10 min pre-treatment of K^+-free solution, the resulting hyperpolarization was recorded in Fig. 30. The amplitude of hyperpolarization increased from 8 mV to 18, 26 mV and 28 mV with increasing K^+ concentration from 1 to 3, 13 mM and 23 mM, respectively.

About the decay rate of hyperpolarization, quantitative comparison was difficult in this experiment but increasing tendency was observed clearly.

Effect of Ca^{++}

If the intracellular Na^+ concentration was related to extracellular Ca^{++} concentration by Na^+/Ca^{++} exchange mechanism, $[Ca^{++}]_o$ might have an effect on Na^+ pump activity.

After 10 minutes pre-treatment with K^+-free Tyrode solution of various Ca^{++} concentration, transient hyperpolarizations in 13 mM K^+-Tyrode solution were observed (Fig. 31). After pretreatment with Ca^{++}-free, K^+-free Tyrode solution, the amplitude of transient hyperpolarization was remark-

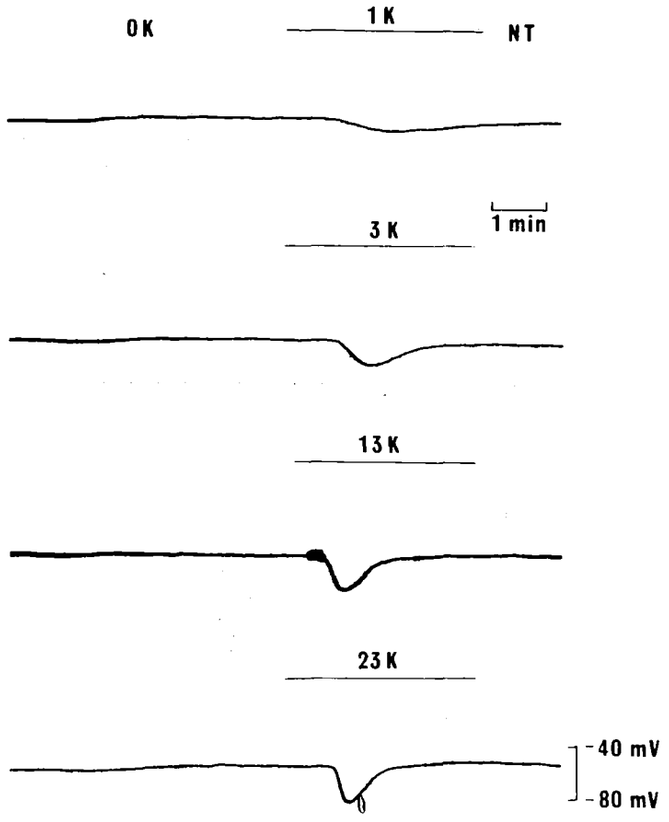

Fig. 30. Effect of K^+ concentration in recovery solution. After pretreatment with K^+-free Tyrode for 10 min, recovery solution with various K^+ concentration (from upper to lower panel 1 mM, 3 mM, 13 mM and 23 mM K Tyrode, respectively) was perfused.

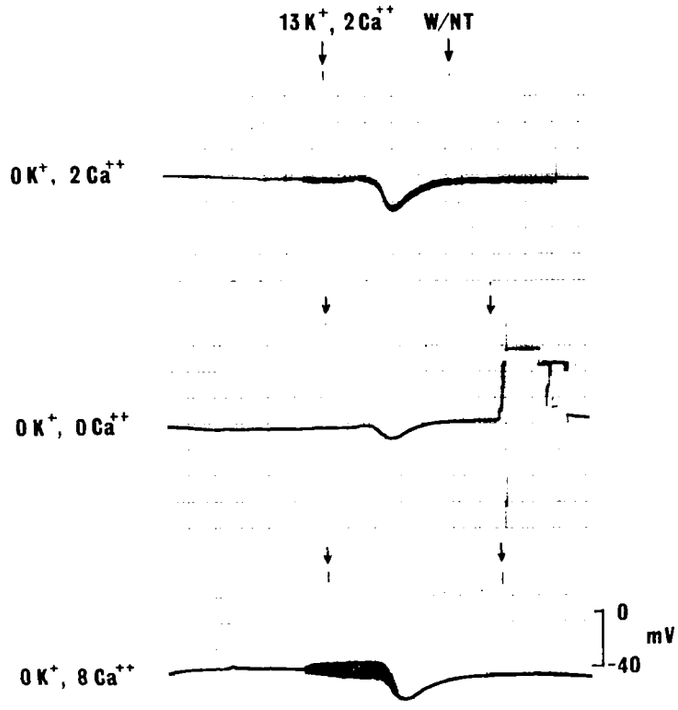

Fig. 31. Effect of Ca^{++} concentration. During the pretreatment with K^+-free Tyrode, Ca^{++} concentration was also varied (upper: 2 mM, Middle: 0 mM, lower: 8 mM). When same recovery solution was perfused, difference in resulting hyperpolarization was noticed.

ably diminished. But in case of 8 mM Ca^{++} and 2 mM Ca^{++}, the differences were not significant.

DISCUSSION

Identification of AV node

By Paes de Carvalho and Almeida (1960) the AV node was divided functionally into three regions: atrionodal (AN), nodal (N) and node-His (NH). Subsequently, some investigators have demonstrated morphologically distinct zones (transitional, midnodal and lower nodal) which appeared to be compatible with those zones described electrophysiologically (DeFelice and Challice 1969), and attempted a direct comparison by performing electrophysiological and morphological studies on the same preparation(Anderson *et al.* 1974). They tried to correlate the activation sequence of the node with its architecture and draw activation map during antegrade and retrograde conduction.

In this study, the area of AV node was decided between the ostium of the coronary sinus and the leaflet of the tricuspid valve. To confirm whether this region was genuine AV node or not, action potential was recorded and compared to typical action potential of AV node. The result revealed that the preparations used in this study were a part of the AV node containing functionally different zones. When the small preparations were used, the zone from which they were removed was not considered.

In two cases, morphological study was performed after electrophysiological study, and nodal cell with histological characteristics of specialized conduction tissue was identified.

Differences between isolated AV node and small preparation

The region in which spontaneous activity of isolated AV node was initiated seemed to be anterior lower node (Fig. 1) or region in the functional aspect. The impulse initiated at this area might be conducted retrograde to AN region through N re-

gion. If spontaneous activity in intact heart is also initiated in NH region (Childers 1977: Moore 1966), it is to be conducted downward to His bundle and at the same time conducted retrograde direction. The effect of the reverse conduction on the cardiac rhythm is not clear yet.

Configuration of action potential and its rate were different in isolated AV node and in small preparation. After dissection of AN node, the rate of beat was increased (from about 60/min to 150/min), the configuration of action potential became similar to that of SA node, and regional difference as shown in isolated AV node was abolished.

Kokubun *et al.* (1980) reported that resting membrane potential decreased after dissection and that it might be attributed by loss of electrical coupling with adjacent tissue which had a more negative resting potential and was expected to hyperpolarize the AV nodal cell. In this experiment, resting membrane potential was not tried to compared in both intact and small preparation but their results suggested a probable explanation that decrease in resting membrane potential should be responsible for increase in the spontaneous discharge rate. Also change in RMP influences the degree of activation in voltage dependent ionic channel, and may cause change in action potential configuration.

In the SA node functional and morphological inhomogeneity have been widely investigated (Masson-Pevet *et al.* 1978). Functonal differences were shown not only in the action potential configuration but also in responses to change in temperature or Ca^{++} concentration and to vagal stimulation (Bouman *et al.* 1978; Mackaay *et al.* 1980). In the AV node, above effects have not been studied, but the regional difference in configuration of action potential was only demonstrated. Whether the regional differences were disappeared after dissection into small preparations was not studied systematically, but the tendency was observed. This result suggested that cell-to-cell interaction in the whole heart should be important in manifesting functional inhomogeneity.

Although the effects resulting from dissection seem to be complex and are not fully understood, preparation of small strips is useful experimental procedure for the electrophysiological study, especially for the voltage clamp technique, and widely used. Therefore, the resulting effects, whether they are advantages or not, must be considered. Firstly, small preparation enables a stable impalement of microelectrode due to minimum contractile movement. Secondly, the membrane potential could be easily controlled by injecting currents through a second intracellular microelectrode. These are important advantages. It is unlikely that membrane structure and properties are changed by dissection, thus there might be no serious problem in studying the membrane channels or ionic mechanism with small preparation.

In the functioning whole heart, there exist probable importance of electrical coupling as well as ionic mechanism (Paes de Carvalho 1983). It might be thought that the small preparation would reveal its intrinsic properties free from the influence of adjacent tissue (Kokubun *et al.* 1980) or that the preparation would lose its intrinsic role in the whole organ. Although it is difficult to directly apply the results obtained from small preparations to the interpretation of the phenomena in the intact AV node or in the whole heart, informations about membrane current system obtained from small preparation could be essential for our understanding of the function of the AV node.

Kinetic study of i_f

The kinetic analysis of i_f was done with the experiment performed in 2 mM Mn^{++}, 13 mM K^+-Tyrode solution. Mn^{++}, which was used as i_{si} blocker because the deactivation process of i_f was usually superimposed on i_{si} activiation, has been known to affect current-voltage relationship for i_f and to increase the magnitude of i_f (Kimura 1982). The effect of K^+ concentration of i_f system was also reported by DiFrancesco (1981a). He proposed increased slope conductance following the increment of K^+ concentration.

Although these ions had effects on i_f itself, 2 mM Mn^{++}, 13 mM K^+-Tyrode solution seemed to be useful for studying i_f. By using this solution, the amplitude of i_f was increased, deactivation of pottassium current which was mixed on i_f activation might be decreased and current tail became clearly noticed. Therefore, the kinetic analysis appeared to be performed relatively easily and could be used widely for studying the underlying mechanism of certain factors which affected i_f.

In this study using 2 mM Mn^{++}, 13 mM K^+-Tyrode solution, current response to the hyperpolarizing pulse seemed to well represent i_f activation from the point of view that it fitted single exponential. Moreover, activation curve and fully activated current-voltage relationship could be obtained successfully by measuring i_{max} and tail amplitude and

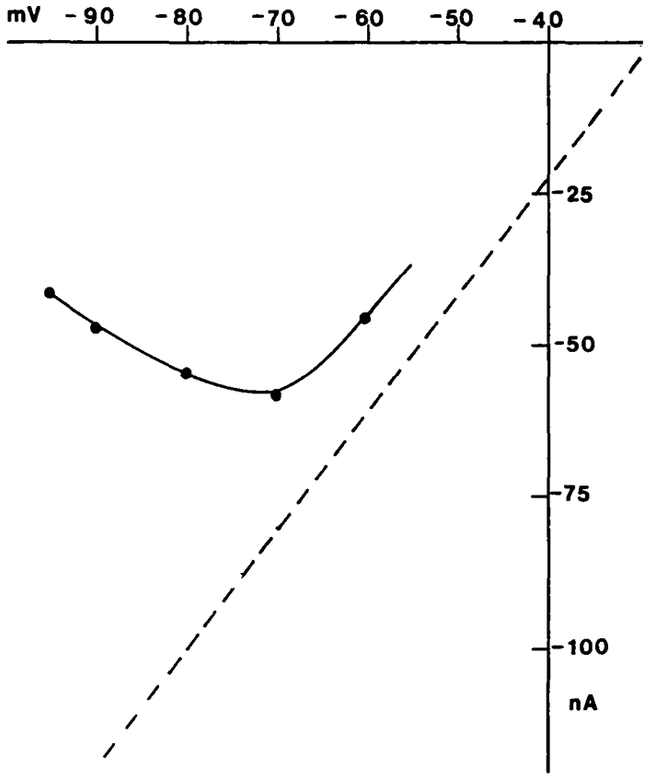

Fig. 32. Voltage dependent blockage of Cs^+ on i_f represented in fully activated I-V relationship. The control curve which was shown in Fig. 20 was drawn by broken line.

by using simple equation.

In the results, i_f in the AV node had similar properties to that in the SA node (Yanagihara and Irisawa, 1980) and that in the Purkinje fibre (DiFrancesco 1981a). But there have been some different results about the reversal potential of i_f. Earm (1983) and Brown *et al.* (1982) proposed more negative value.

Voltage dependent blockage of Cs^+ on i_f

Perfusion with 0.5 mM Cs^+ reduced the current activated during the negative pulse. The more the pulse was negative, the more the current was reduced. However the tail was less affected after the larger pulse. The result suggested that Cs^+ induced blockage was voltage-dependent.

Further description of voltage-dependence of Cs^+ action was given by plotting activation curve and fully activated I-V relationship.

As shown in Fig. 32, fully activated I-V relationship showed current depression which increased with the membrane polarizaiton. According to the single-ion channel model of Woodhull (1973), the phenomenon was considered to be explained by assuming that the blocking ion entered the channel and ran a fraction of membrane thickness before blocking the channel itself. At more negative voltage, the probability that the inner site occupied by the blocking ion was augmented, and the current reduced progressively with negative membrane potential.

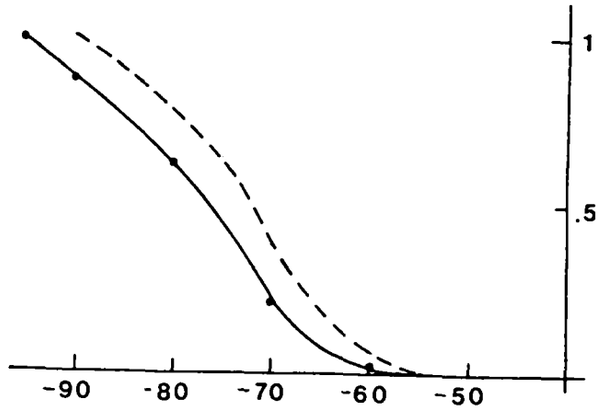

Fig. 33. Effect of Cs^+ on activation curve of i_f. Broken line: the control curve shown in Fig. 19.

Cs^+-induced blockage of K^+-permeable channels has been extensively investigated in skeletal muscle (Gay and Stanfield 1977), the node of Ranvier (Dubios and Bergman 1977) and the squid axon (Adelman and French 1978). In cardiac muscle Cs^+ has been known to have blocking action of i_f in Purkinje fibre and the SA node (DiFrancesco and Geda 1980; DiFrancesco 1981b) and its voltage dependent manner was fully studied by DiFrancesco (1982). He reported the i_f current reduction at negative potential similar to our result, and insisted that the current became larger in the far positive range. He also suggested acceleration of the time course of activation in Cs^+. But time course seemed to be decelerated by 0.5 mM Cs^+ in this study.

Furthermore, the slope of activation curve appeared to decrease as shown in Fig. 33, and the potential at which 50% activation was achieved became more negative by about 5 mV than control. This result suggested that Cs^+ influenced the voltage dependence of the gate molecule as well as blocked the channel.

Recovery from the inactivation for i_{si}

It has been noticed that in the AV nodal cell recovery of excitability was delayed well beyond repolarization and that frequency-dependent de-

pression of nodal conductivity was related to cumulative effects upon excitability (Merideth *et al.* 1968). Because the AV nodal action potential was mainly contributed by slow inward current, excitability seemed to be related to the activation state of i_{si} and recovery of excitability to the recovery of i_{si} from inactivation.

Recovery time course was proved to be much longer than inactivation time course in the ventricular muscle fibre by Kohlhardt *et al.* (1975). Then, they proposed the third gating parameter which was inactivated and reactivated later than gate f. This seemed to be also the case in this study. The time constant of recovery process was 270 msec, which was similar to the result of Kohlhardt *et al.* (1975). And significant amount of inactivation remained at 500 msec after returning to holding potential, which seemed to be related to the fact that diastolic threshold was not attained in nodal cell until 0.2 to 0.5 seconds after restoration of resting membrane potential (Merideth *et al.* 1968)

Pump current

In this experiment, Na/K activated pump was identified by electrophysiological manner in the AV node. It could hyperpolarize membrane potential over 30 mV depending upon a situation.

The effect of K^+ concentration in recovery solution on transient hyperpolarization was studied by Eisner and Lederer (1980) and Gadsby (1980).

They showed that the decay rate constant of the electrogenic Na^+ pump current transient depended on extracellular K^+ concentration and was a good measure of the degree of activation of external site of the Na^+ pump. The decay rate of hyperpolarization tended to increase in this experiment but the difference was too small for quantitative analysis.

Gadsby (1980) reported the pump was half-maximally activated by about 1 mM K^+. In this experiment 1 mM K^+ was not enough to activate pump to that extent.

Pacemaker mechanism

Since the decay of a Na^+ outward current in combination with the inward background current was suggested as the basis for the pacemaker depolarization in Purkinje fibre (Dudel and Trautwein 1958; Vassalle 1966), every current system has been considered to be able to participate in the generation of the pacemaker potetial (Yanagihara and Irisawa 1980). But which current system is mainly contributing to pacemaker activity is not yet clarified.

The importance of i_{si} in generation of the pacemaker depolarization has been emphasized by Irisawa's group (Irisawa and Noma 1982; Noma *et al.* 1980; Yanagihara and Irisawa 1980). They insisted that i_{si} took an active role in the latter half of the pacemaker depolarization and their computer model suggested the presence of i_{si} during the entire diastolic depolarization. They also suggested i_{si} mediate the positive chronotropic effect of epinephrine.

On the other hand, Brown and DiFrancesco (1980) presented experimental evidence that i_f was important not only in normal pacemaking but also in mediating the acceleratory effects of adrenaline and temperature.

Noble (1984) proposed that i_k inactivation had a key role for the pacemaker depolarization in the SA node, and i_f and other background inward current systems played supporting actions on it.

In this experiment pacemaker mechanism in spontaneously active AV nodal cell was not directly investigated. Considering the similarity between SA node and AV node (low resting membrane potential, pacemaker depolarization, slow action potential), it is suggested that pacemaker mechanism should also be similar in both tissue.

The extent of contribution of i_{si} and i_f was studied indirectly by comparing the effect of adrenaline on i_{si} and i_f (Fig. 13, 23). Considering the fact that the amplitude of i_f in normal Tyrode solution was small in pacemaker range and was little increased by adrenaline, i_f did not seem to play a significant role in pacemaking and mediating chronotropic effect of adrenaline in the AV node. In contrast, i_{si} was increased remarkably and seemed to be important in positive chronotropic effect of adrenaline. However, this cannot be a general conclusion because there may exist regional differences in current amplitude and adrenaline effect.

REFERENCES

Adelman WJ, French RJ. Blocking of the squid axon potassim channel by external caesium ions. J. Physiol. 1978, 276:13-25

Anderson RH, Janse MJ, van Capelle JL. A combined morphological and electrophysiological study of the atrioventricular node of rabbit heart. Circ. Res. 1974, 35:909-922

Beeler GW, Reuter H. Membrane calcium current in ventricular myocardial fibres. J. Physiol. 1970, 207:191-209

Bouman LN, Mackaay AJC, Bleeker WK, Becker AE. Pacemaker shifts in the sinus node. Effects of vagal stimulation, temperature and reduction of extracellular calcium. In Bonke FIM (Ed) The sinus node. Nijhoff, Hague Netherlands, 1978: pp. 245-157

Brown HF, DiFrancesco D. Voltage clamp of membrane currents underlying pacemaker activity in rabbit sinoatrial node. J. Physiol. 1980, 308:331-351

Borwn HF, DiFrancesco D, Noble SJ. How does adrenaline 'accelerate the heart? Nature 1979, 280: 325-236

Brown HF, Kimura J, Noble SJ. The relative contribution of various time-dependent membrane currents to pacemaker activity in the sinoatrial node. In Bouman LN, Jongsma HJ (Ed) Cardiac rate and rhythm. Nijhoff, Hague, 1982: pp. 53-68

Brown AM, Lee KS, Powell T. Sodium current in single rat heart muscle cells. J. Physiol. 1981, 318:479-500

Childers R. The AV node; Normal and abnormal physiology. Prog. In Cardiovasc. Dis. 1977, 19(5):316-384

Colatsky TJ. Voltage clamp measurements of sodium channel properties in rabbit cardiac Purkinje fibres. J. Physiol. 1980, 305:215-234

Coraboeuf E. Voltage clamp studies of the slow inward current. In Zipes DP, Bailey JC, Elharrar V (Ed) The slow inward current and cardiac arrhythmias. Nijhoff, Hague Netherlands, 1978: pp. 25-96

DeFelice LJ, Challice CE. Anatomical and ultrasturctural study of the electophysiological atroventricular node of the rabbit. Circ. Res. 1969, 24:457-474

DeMello WC. Passive electrical properties of the atrioventricular node. Pflügers Arch. 1977, 371: 135-139

DiFrancesco D. A study of the ionic nature of the pace-maker current in calf Purkinje fibres. J. Physiol. 1981a, 314:377-393

DiFrancesco D. A new interpretation of the pace-maker current in calf Purkinje fibres. J. Physiol. 1981b, 314:359-376

DiFrancesco D. Block and activation of the pacemaker channel in calf Purkinje firbres: Effects of potassium, caesium and rubidium. J. Physiol. 1982. 329:485-507

Dubois JM, Bergman C. The steady-state potassium coductance of the Ranvier node at various external K^+-concentrations. Pflügers Arch. 1977, 370:185-194

Earm YE. The kinetics of hyperpolarization activated current (i_f) in sinoatrial node of the rabbit. Kor. J. Physiol. 1980, 41:441-474

Gadsby DC. Activation of electrogenic Na^+/K^+ exchange by extracellular K^+ in canine cardiac Purkinje fibers. Proc. Natn. Acad. Sci. U.S.A. 1980, 77:7035-7039

Gay L, Stanfield PR. Ca^{++} causes a voltage-dependent block of inward K^+ currents in resting skeletal muscle fibres. Nature. 1977, 267:169-170

Hoffman BF. Paes de Carvalho A, DeMello WC. Transmembrane potentials of single fibres of the atrioventircular node. Nature. 1958, 181:66-67

Hoffman BF, Paes de Carvalho A, DeMello WC, Cranefield PF Electrical activity of single fibres of the atrioventricular node. Circ. Res. 1959, 7:11-18

Irisawa H, Noma A. Pacemaker Mechanism of rabbit sinoatrial node cells. In Bouman LN, Jongsma HJ (Ed) Cardiac rate and rhythm. Nijhoff, Hague, 1982: pp. 35-52

Isenberg G, Klöckner U. Calcium currents of isolated bovine ventricular myocytes are fast and of large amplitude. Pflügers Archiv. 1982, 395:30-41

Keynes RD, Swan RO. The permeability of frog muscle fibres to lithium ion. J. Physiol. 1959, 147:626-638

Kimura J. Electrophysiological studies of the sino-atrial node of the rabbit. 1982, D. Phil. thesis, Oxford, Oxford University

Kohlhardt M, Drause H, Kubler M, Herdey A. Kinetics of inactivation and recovery of the slow inward current in the mammalian ventricular myocardium. Pflügers Arch. 1975, 355:1-17

Kokubun S, Nishimura M, Noma A, Irisawa H. The spontaneous action potential of the rabbit atrioventricular node cells. Jpn. J. Physiol. 1980, 30:529-540

Kokubun S, Nishimura M, Noma A, Irisawa H. Membrane currents in the rabbit atrioventricular node cell. Pflügers Arch. 1982, 393:15-22

Leclercq JE, Coumel P. The role of the AV node in supraventricular tachycardia. In Rosenbaum MB, Elizare MV (Ed) Frontiers of cardiac electrophysiology. Nijhoff, Hague, Netherlands, 1983: pp. 376-396

Lieberman M, Kootsey JM, Johnson EA, Sawanobori T. Slow conduction in cardiac muscle: A biophysical model. Biophys. J. 1973, 13:37-55

Mackaay AJC, Bleeker WK, Po't Hof T, Bouman LN. Temperture dependence of the chronotropic actions of calcium and functional inhomogeneity of the rabbit sinus node. J. Mol. Cell. Cardiology. 1980, 12(5):433-443

Masson-Pévet M, Bleeker WK, Mackaay AJC, Gros D, Bouman LN. ULtrastructural and functuonal aspects of the rabbit sino-atrial node. In Bonke FIM (Ed) The sinus node. Nijhoff, Hague, Netherlands 1978: pp. 245-257

Medez C, Moe GK, Mueller WH, Moe GK. Electrical excitability of atrioventricular nodal cells. Circ. Res. 1968, 23; 69-85

Moore RN. Microelctrode studies on concealment of multiple premature atrial responses. Circ. Res. 1966, 18:660-672

Noble D. The surprising heart; A review of recent progress in cardiac electrophysiology. J. Physiol. 1984, 353:1-50

Noma A, Kotake H, Irisawa H. Slow inward current and its role mediating the chronotropic effect of epinephrine in the rabbit sinoatrial node. Pflügers Archiv. 1980,

388:1-9

Noma A, Yanagihara K, Irisawa H. Inward current of the rabbit sinoatrial node cell. Pflügers Archiv. 1977, 372:43-51

Paes de Carvalho A, de paula Carvalho M. Propagation throgh the atrioventricular node. In Rosenbaum MB, Elizari MV (Ed) Frontiers of cardiac electrophysiology. Nijhoff, Hague, Netherlands, 1983: pp. 349-356

Pollack GH. Intercellular coupling in the atrioventricular node and other tissues of the rabbit heart. J. Physiol. 1976, 255:275-298

Rougièr O, Vassort G, Garnier D, Gargouil YM, Coraboeuf E. Existence and role of a slow inward current during the frog atrial action potential. Pflügers Arch. 1969, 308:91-110

Ruiz-Cerretti E, Ponce Zumino A, Parixii IM. Resolution of two components in the upstroke of the action potential in atrioventricular fibers of the rabbit heart. Can. J. Physiol. Pharmacol. 1971, 49:642-648

Son BK. Effects of ions, neurotransmitters, local anesthetics and Ca^{++}-blockers on the spontaneous action potential of the atrioventricular node in the rabbit. 1985, Ph. D. thesis, Seoul National University.

Ten Eick R, Nawrath R, McDonald TF, Trautwein W. On the mechanism of the negative inotropic effect of acetylcholine. Pflügers Arch. 1976, 361:207

Thomas RC. Intracellular sodium activity and the sodium pump in snail neurons. J. Physiol. 1972, 220:55-71

Vassalle M. Analysis of cardiac pacemaker potential using a voltage clamp technique. Am. J. Physiol. 1966, 210:1335-1341

Watanabe Y, Dreifus LS. Sites of impulse formation within the atrioventrcular junction of the rabbit. Circ. Res. 1968, 22:717-727

Wit AS, Cranefield PF. Effect of verapamil on the sinoatrial and mechanism by which it arrests reentrant atrioventricular nodal tachycardia. Circ. Res. 1974, 35:413-425

Woodhull AM. Ionic blockage of sodium channels in nerve. J. Gen. Physiol. 1980, 385:11-19

Yanagihara K, Irisawa H. Inward current activated during hyperpolarization in the rabbit sinoatrial node cell Pflügers Archv. 1980, 385:11-19

Zipes DP, Mendez C. Action of manganese ion and tetrodotoxin on atriovetricular nodal transmembrane potentials in isolated rabbit hearts. Circ. Res. 1973, 447-454

= 국문초록 =

방실결절의 세포막 이온전류에 관한 연구

서울대학교 의과대학 생리학교실

호원경 · 김우겸 · 엄융의

방실결절은 동방결절에서 시작된 흥분이 심실로 전달되는 유일한 통로로서 뿐만 아니라 자동능을 나타낼 수도 있어서 방실결절의 활동전압과 그의 전도 기전은 심장의 기능을 이해하는데 있어 매우 중요하게 생각되어 왔으나 근본적인 기전에 관한 연구는 1980년 Kokubun 등이 방실결절의 작은 절편에 두개의 유리미세전극을 이용한 막전압고정법을 적용하면서 비로소 시작되었다.

본 연구에서는 방실결절을 적출하여 자발적 활동전압을 기록하고 그 전도양상을 관찰하였고, 방실결절에 존재하는 이온 전류를 밝히기 위하여 적출 방실결절을 폭 0.3 mm의 작은 조각으로 만들어 막전압고정법을 시행하여 다음과 같이 결과를 얻었다.

1. 적출 방실결절은 자발적 활동전압을 나타내었고, 빈도는 50—60/분으로 동방결절에 비해 느렸다. 활동전압의 모양은 전형적인 방실결절의 활동전압으로 보고된 것들과 같았으며 부위별로 차이를 볼 수 있었다.

2. 방실결절을 작은 절편으로 만든 뒤에도 대부분 자발적 활동전압이 관찰되었고 빈도는 평균 150/min으로 빨라졌으며, 그 모양은 동방결절의 활동전압과 유사하여져서 적출 방실결절에서보다 큰 pacemaker potential을 보였다.

3. 방실결절의 작은 절편에 미세전극 두개로 막전압고정법을 시행하여 저분극에 의해 활성화되는 완만내향전류, i_{si}와 과분극에 의해 활성화되는 내향전류, i_f의 동력학적 성상을 분석하였다.

4. i_{si}는 —25 mV 부근에서 활성화되기 시작하여 —15 mV에서 가장 큰 크기를 보였고 2 mM Mn^{++}에 의해 소실되었으며 10^{-6}M adrenaline을 가하자 그 크기가 현저히 증가하였다. inactivation gate, f의 활성화곡선은 S자형으로 —26 mV에서 50% activation을 보였다. inactivation에서 회복되는 경과를 관찰하였는데 시정수는 270 msec였다.

5. 정상 Tyrode용액에서 활성화되는 i_f는 크기가 작아서 i_f의 특성을 연구하기 위한 실험은 2 mM Mn^{++}, 13 mM K^+-Tyrode용액에서 하였다. i_f는 —70 mV 이하에서 활성화되기 시작하였고 과분극이 커질수록 그 크기가 커졌으며 역전전압은 —25 mV였다. i_f는 10^{-6}M adrenaline에 의해서는 별 영향을 받지 않았고, 0.5 mM Cs^+에 의하여 현저히 감소되었다.

6. K-free Tyrode로 10분간 전처치한 후 13 mM K^+-Tyrode용액을 관류하여 Na^+pump의 활성화에 의해서 나타나는 일과성 외향전류와 일과성과분극을 관찰하였다. 일과성과분극의 크기는 전처치의 기간이 길수록, 전처치 후 관류액의 K^+ 농도가 높을수록 커졌으며, K^+-free Tyrode 용액의 Ca^{++} 농도를 낮추면 작아졌다.